Hole-conductor-free perovskite organic lead iodide heterojunction thin-film solar cells: High efficiency and junction property

Jiangjian Shi, Juan Dong, Songtao Lv, Yuzhuan Xu, Lifeng Zhu, Junyan Xiao, Xin Xu, Huijue Wu, Dongmei Li, Yanhong Luo, and Qingbo Meng[a)]

Key Laboratory for Renewable Energy, Chinese Academy of Sciences, Beijing Key Laboratory for New Energy Materials and Devices, Institute of Physics, Chinese Academy of Sciences, Beijing 100190, People's Republic of China

(Received 15 December 2013; accepted 23 January 2014; published online 10 February 2014)

Efficient hole-conductor-free organic lead iodide thin film solar cells have been fabricated with a sequential deposition method, and a highest efficiency of 10.49% has been achieved. Meanwhile, the ideal current-voltage model for a single heterojunction solar cell is applied to clarify the junction property of the cell. The model confirms that the $TiO_2/CH_3NH_3PbI_3/Au$ cell is a typical heterojunction cell and the intrinsic parameters of the cell are comparable to that of the high-efficiency thin-film solar cells. © *2014 AIP Publishing LLC*. [http://dx.doi.org/10.1063/1.4864638]

Perovskite organic lead halide compounds (e.g., $CH_3NH_3PbX_3$, X = I, Br, and Cl) as light absorbers have shown promising performance for thin film solar cells,[1–6] hopeful to acting with Si, Cu(In, Ga)Se_2, or $Cu_2ZnSn(S, Se)_4$ to form hybrid tandem solar cells.[7] By cooperating with Spiro-OMeTAD as hole transport material (HTM), perovskite organic lead halide based solid-state thin film solar cells have already exhibited high power conversion efficiency (PCE) beyond 15%.[2–4]

However, compared to other components, the use of HTMs bears a large proportion of cost for such solar cells, limiting their approach to low-cost photovoltaic devices.[8] Therefore, it is worth developing low-cost HTMs or developing and improving the performance of HTM-free solar cells. The HTM-free solar cell has a much simpler structure benefiting for reducing the cost. With efforts on the photoanode and back contact interfacial modification, a PCE in the range of 5%–8% has been achieved.[5,6,9] Etgar and his colleagues developed an efficient absorber deposition method with combination of different solvents, yielding a PCE of 8.04%.[6] Conventionally, the cell based on organic lead halides and nanoporous TiO_2 layer is thought to be a sensitized solar cell though the organic lead halides themselves can transport carriers.[2,4] Therefore, a controversy still exists whether it is a sensitized or a heterojunction solar cell,[6] though it has a structure more like Cu(In,Ga)Se_2 and $Cu_2ZnSn(S,Se)_4$ heterojunction solar cells. It is worth noting that a Mott-Schottky analysis has been employed to explain the junction property of the cell.[6] However, besides accurately measuring the capacitance properties, more independent works are needed to obtain a confirmation on the working mechanism of the cell.

In this work, a series of efficient $TiO_2/CH_3NH_3PbI_3/Au$ solar cells has been fabricated with a sequential deposition method and a model completely based on the heterojunction solar cell was employed to clarify the working mechanism of the cell and the controversy mentioned above. Further investigation reveals that our cells agree well with the ideal model for single heterojunction solar cells and some intrinsic parameters of the cell have also been obtained.

With two-step sequential deposition method,[2,10,11] a series of efficient solar cells with a structure as depicted in Figure 1(a) has been fabricated,[12] the PCEs of which are shown in Figure 2(a) as a histogram. The highest PCE of 10.49% has been achieved with open-circuit voltage (V_{OC}) of 905 mV, short-circuit current density (J_{SC}) of 17.8 mA/cm^2, and fill factor (FF) of 0.65 (Figure 2(b)).

Typical current-voltage (*I-V*) characteristics of the cell measured at illumination (AM 1.5, light intensity of 100 mW/cm^2) and in dark for further analysis are shown in Figure 3(a). The PCE is 8.72% with V_{OC} of 0.81 V, J_{SC} of 14.51 mA/cm^2, and FF of 0.74. In dark, the current density of the cell keeps about zero when the voltage is lower than 0.6 V and drops gradually when the voltage further increases, in good agreement with the *I-V* curve at illumination and implying that the shunt resistance of the cell is very large. To further clarify the photovoltaic characteristics, a model based on the single heterojunction solar cell is put forward to analyze the *I-V* property of the cell. According to the equivalent circuit in Figure 1(b), the *I-V* characteristic of a single heterojunction solar cell is described as[13,14]

$$J = J_L - J_0\left[\exp\left(\frac{e(V + J \times R_S)}{AK_BT}\right) - 1\right] - \frac{V + J \times R_S}{R_{sh}}, \quad (1)$$

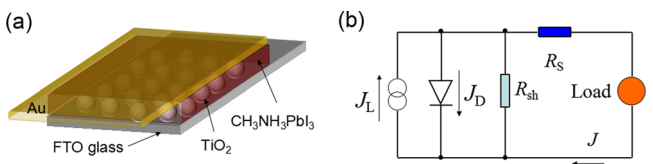

FIG. 1. (a) Scheme of $TiO_2/CH_3NH_3PbI_3/Au$ heterojunction solar cells, (b) ideal model for single heterojunction solar cells with J_L (the light induced constant current), J_D (the current of PN junction diode), R_S (the series resistance), R_{sh} (shunt resistance), and J (the current flowing through the external load).

[a)]Author to whom correspondence should be addressed. Electronic mail: qbmeng@iphy.ac.cn

 © 2014 AIP Publishing LLC

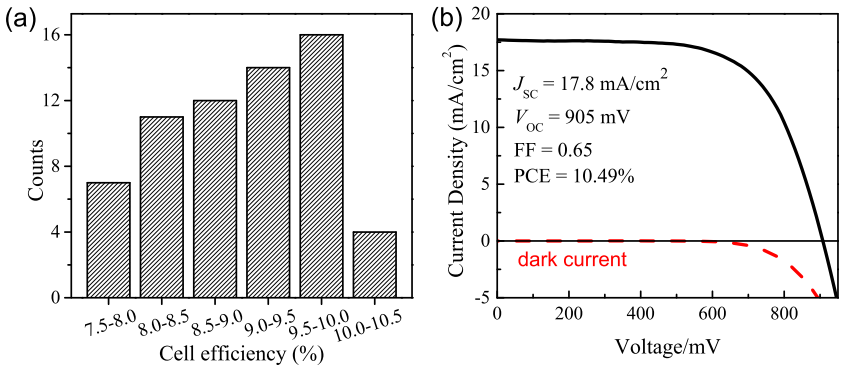

FIG. 2. (a) Histogram plot of the cell performance and (b) *I-V* curves of the best performed cell.

where J_L is the light induced constant current density, J_0 is the reverse saturated current density of a PN heterojunction, R_S is the series resistance, R_{sh} is the shunt resistance, J is the current density flowing through the external load, A is the ideality factor of a heterojunction, K_B is the Boltzmann constant, T is the absolute temperature, e is the elementary charge, and V is the DC bias voltage that applied at the cell. Some intrinsic parameters of the cell can be derived from Eq. (1) for an ideal heterojunction solar cell. It can be deduced (R_{sh} is very large)

$$-\frac{dV}{dJ} = \frac{AK_BT}{e}(J_{SC} - J)^{-1} + R_S, \tag{2}$$

$$\ln(J_{SC} - J) = \frac{e}{AK_BT}(V + R_S \times J) + \ln J_0. \tag{3}$$

Figure 3(b) gives the plots of $-dV/dJ$ vs $(J_{SC}\text{-}J)^{-1}$ and the linear fitting curves according to Eq. (2). It can be found that there is a good linear relationship between $-dV/dJ$ and $(J_{SC}\text{-}J)^{-1}$ both at illumination and in dark, which means that the cell we fabricated is a well-behaved heterojunction solar cell to a certain extent.[13] The ideality factor and series resistance of the cell are derived from the slope and intercept of the linear fitting results, as shown in Figure 3(b). Under illumination, the ideality factor is 1.88 and the series resistance is 1.31 Ω cm^2, while in dark the ideality factor is 1.93 and the series resistance is 4.25 Ω cm^2. In a heterojunction solar cell, values of the ideality factor represent the quality of a junction and the carrier recombination mechanisms.[13,14] For a well-behaved heterojunction solar cell, the ideality factor is typically in the range $1.3 < A < 2$. When the diode current of a PN junction is dominated by the carrier diffusion in the neutral region of semiconductors, A is approaching 1. On the other hand, when carrier recombination in depleted space-charge region dominates the diode current, A is approaching 2. In most cases, both carrier diffusion and recombination take place simultaneously and $1 < A < 2$.[14] In our case, both the ideality factors at illumination and in dark is larger than 1.3 and the difference (0.05) between them is relatively small, both of which indicate that the cell agrees well with the heterojunction solar cell model and there is a good agreement between dark and illuminated conditions. Furthermore, the

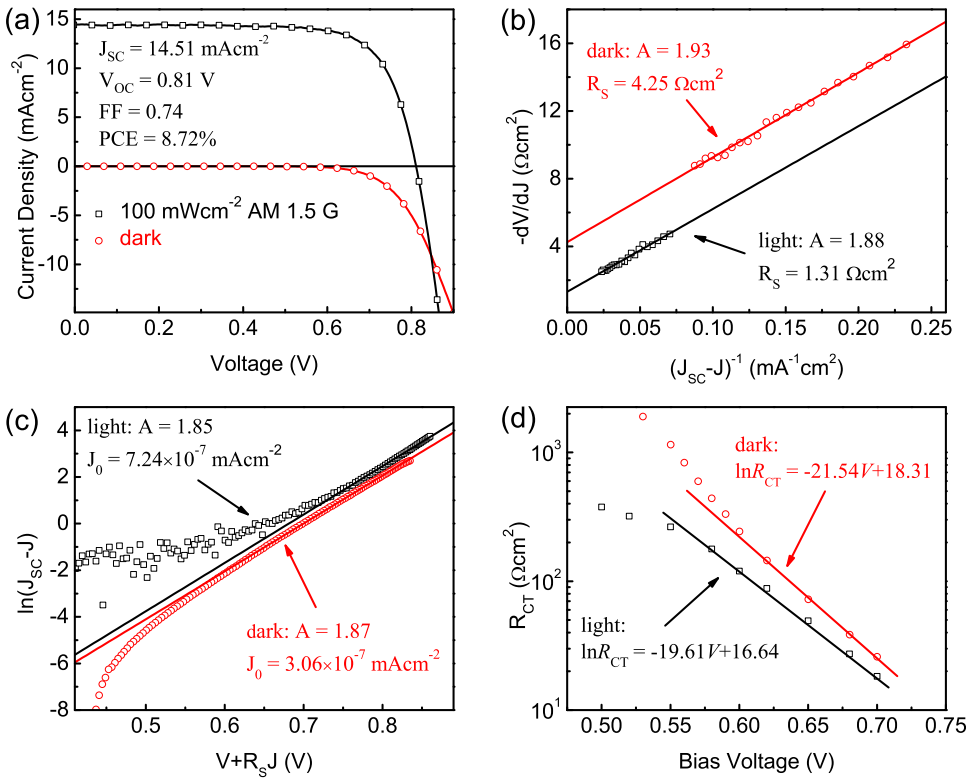

FIG. 3. (a) Current-voltage characteristics, (b) plots of $-dV/dJ$ vs $(J_{SC}\text{-}J)^{-1}$ and the linear fitting curves, (c) plots of $\ln(J_{SC}\text{-}J)$ against $V + R_S J$ and the linear fitting curves, (d) plots of charge recombination resistance (R_{CT}) against the bias voltage and the fitting curves of the cell under AM 1.5 illumination (100 mW/cm^2) and in dark, respectively.

series resistance at illumination is very small, which can be comparable to the highly performed CdTe[14] and $Cu_2ZnSn(S,Se)_4$[15–17] thin film solar cells. As we know, a small series resistance is necessary for a high-performance solar cell with a high fill factor according to Eq. (1).[16]

Figure 3(c) gives the plots of $\ln(J_{SC}\text{-}J)$ vs. $V + R_S J$ and there is also a linear relationship between them. The ideality factor and reverse saturated current density are also derived from the linear fitting results, as in Figure 3(c). The values of ideality factor in dark and under illumination are 1.87 and 1.85, respectively, which is very close to that derived from Figure 3(b). The relatively large ideality factors both in dark and under illumination indicate that the diode current is mainly controlled by recombination in the space charge region of the TiO_2 and $CH_3NH_3PbI_3$ layers,[13] which confirms the existence of a depletion region in the cell, agreeing with Etgar's result.[6] The reverse saturated current density of the cell under illumination and in dark is 7.24×10^{-7} mA/cm^2 and 3.06×10^{-7} mA/cm^2, respectively, which is also comparable to those of $Cu(In,Ga)Se_2$[13,18] and $Cu_2ZnSn(S,Se)_4$[15,17] thin film solar cells. According to Eq. (1), when R_{sh} is large enough, the V_{OC} of a heterojunction solar cell can be deduced as

$$V_{OC} = \frac{AK_BT}{e}\ln\left(\frac{J_L + J_0}{J_0}\right) \approx \frac{AK_BT}{e}\ln\left(\frac{J_{SC}}{J_0}\right). \quad (4)$$

It is obvious that the V_{OC} is determined by the ideality factor, working temperature, light-induced current, and the reverse saturated current of the cell, while a low J_0 together with a large ideality factor is needed for a high V_{OC}. With the parameters of the cell shown in Figures 3(b) and 3(c), the ideal V_{OC} of the cell is calculated to be 0.82 V ($A = 1.865$), which is very close to the experimental result. All the analyses above reveal that a quasi-ideal heterojunction thin film solar cell with the sequential method has been fabricated.

The cell parameters can also be obtained from impedance spectra cooperating with the model of the cell. When a perturbation bias is applied at the cell, the current response can be derived with Eq. (1), thus deducing the charge recombination resistance (R_{CT})[19]

$$R_{CT} = \eta \times \exp\left(-\frac{eV}{AK_BT}\right), \quad (5)$$

where η is a pre-exponential factor. Equation (5) indicates that the R_{CT} (derived from the impedance spectra) decreases exponentially with increasing the DC bias voltage. Figure 3(d) gives the plots of R_{CT} vs. the DC bias voltage and the fitting results. According to the fitting results, the ideality factors can be induced as $A = 1.96$ and $A = 1.78$ under illumination and in dark, respectively. We can see that there is a good agreement in the values of ideality factor with different measurements, and it can be inferred that all the results are reliable.

To further analyze the light-to-electricity conversion ability of the cell in Figure 3 at varied wavelengths, the monochromatic incident photon-to-electron conversion efficiency (IPCE) spectrum[20,21] is given in Figure 4(a). The IPCE reaches a maximum value of about 70% at 500 nm, whereas gradually drops at longer wavelengths, consistent with the absorption of the $CH_3NH_3PbI_3$ layer at varied wavelengths. The integral of the IPCE can get a J_{SC} of 13.8 mA/cm^2, close to the *I-V* result in Figure 3. Internal quantum efficiency (IQE) can directly present the carrier collection ability of the cell without being affected by the absorption,[2] which is shown in Figure 4(b). A maximum value still appears at 500 nm, then the IQE drops gradually, suggesting that the carrier collection ability in the deeper region of the $CH_3NH_3PbI_3$ layer is not as strong as that in the shallow region due to carrier recombination in the neutral region.[9,22] Figure 4(c) gives the plots of J_{SC} vs. incident light intensity to illuminate the carrier transport properties of the cell. It is obvious that there is a linear relationship between J_{SC} and light intensity, which means that carriers can transport smoothly in the semiconductors and there is no obvious difference in the transport velocity between electrons and holes.[23–25] It is in agreement with the measuring results of carrier diffusion constants of $CH_3NH_3PbI_3$[26,27] and previous experimental results in the literature.[4]

The above analyses reveal that $TiO_2/CH_3NH_3PbI_3$/Au is a typical heterojunction solar cell, in which the n-type wide-band-gap TiO_2 acts as a window layer, and the $CH_3NH_3PbI_3$ acts as an absorber layer. Moreover, the cell parameters including the ideality factor, the series resistance, and the reverse saturated current are comparable to that of the high-efficiency thin film solar cells (CdTe, $Cu(In,Ga)Se_2$, and $Cu_2ZnSn(S,Se)_4$). However, the performance is still lower than them, especially in the J_{SC}. For an ideal heterojunction thin film solar cell, the absorber should have wide-range absorption, high carrier collection, and transport efficiency with low recombination. In Cu(In, Ga)Se_2 thin film solar cells, high-quality Cu(In, Ga)Se_2 crystals, appropriate interface manipulation, accurate regulatory of

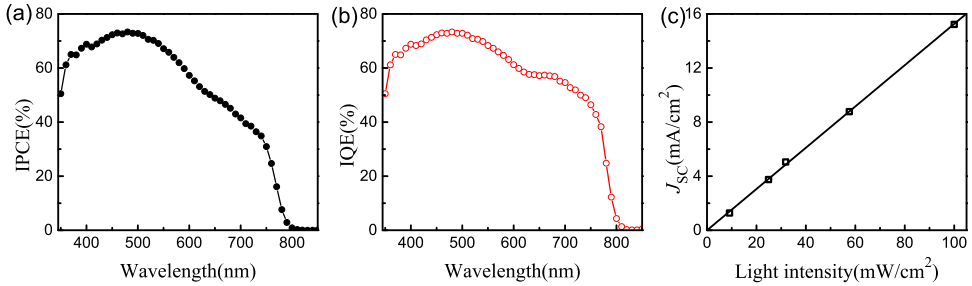

FIG. 4. (a) IPCE spectrum, (b) IQE spectrum derived from the IPCE and absorption spectrum, and (c) short-circuit current density (J_{SC}) as a function of incident light intensity.

components, and well-designed energy band structure are the key to their high performance.[28] Since the organic lead iodide based HTM-free solar cells have been demonstrated to be typical heterojunction solar cells with Mott-Schottky[6] and the *I-V* analysis, these mature technologies used in $Cu(In, Ga)Se_2$, $Cu_2ZnSn(S, Se)_4$, and Si solar cells could also be employed to improve the cell performance.[9]

In conclusion, a series of efficient $TiO_2/CH_3NH_3PbI_3/Au$ solar cells have been fabricated with a sequential deposition method, and a highest efficiency of 10.49% has been achieved. The ideal model for a single heterojunction solar cell has been applied to clarify the cell characteristics and some self-consistent cell parameters have also been derived. The model confirms that the $TiO_2/CH_3NH_3PbI_3/Au$ is a typical heterojunction solar cell. Meanwhile, the cell parameters derived from the model indicate that the performance of the cell is comparable to that of the high-efficiency thin-film solar cells.

This work was supported by Beijing Science and Technology Committee (No. Z131100006013003), National Key Basic Research Program (No. 2012CB932903), and Natural Science Foundation of China (Nos. 21173260 and 91233202). The authors also thank Ms. Li Chunhui and Mr. Luo Jianheng for measurements of solar cells and scientific discussions.

[1]A. Kojima, K. Teshima, Y. Shirai, and T. Miyasaka, J. Am. Chem. Soc. **131**, 6050 (2009).
[2]J. Burschka, N. Pellet, S. J. Moon, R. H. Baker, P. Gao, M. K. Nazeeruddin, and M. Grätzel, Nature **499**, 316 (2013).
[3]M. M. Liu, B. Johnston, and H. J. Snaith, Nature **501**, 395 (2013).
[4]H.-S. Kim, C.-R. Lee, J.-H. Im, K.-B. Lee, T. Moehl, A. Marchioro, S.-J. Moon, R. Humphry-Baker, J.-H. Yum, J. E. Moser, M. Grätzel, and N.-G. Park, Sci. Rep. **2**, 591 (2012).
[5]L. Etgar, P. Gao, Z. Xue, Q. Peng, A. K. Chandiran, B. Liu, M. K. Nazeeruddin, and M. Grätzel, J. Am. Chem. Soc. **134**, 17396 (2012).
[6]W. A. Laban and L. Etgar, Energy Environ. Sci. **6**, 3249 (2013).
[7]H. J. Snaith, J. Phys. Chem. Lett. **4**, 3623 (2013).
[8]N. J. Jeon, J. Lee, J. H. Noh, M. K. Nazeeruddin, M. Grätzel, and S. Seok II, J. Am. Chem. Soc. **135**(51), 19087–19090 (2013).
[9]J. Shi, W. Dong, Y. Xu, C. Li, S. Lv, L. Zhu, J. Dong, Y. H. Luo, D. M. Li, Q. B. Meng, and Q. Chen, Chin. Phys. Lett. **30**, 128402 (2013).
[10]K. Liang, D. B. Mitzi, and M. T. Prikas, Chem. Mater. **10**, 403 (1998).
[11]D. Bi, L. Häggman, G. Boschloo, L. Yang, E. M. J. Johansson, M. K. Nazeeruddin, M. Grätzel, and A. Hagfeldt, RSC Adv. **3**, 18762 (2013).
[12]See supplementary material at http://dx.doi.org/10.1063/1.4864638 for the experimental and characterization details.
[13]S. S. Hegedus and W. N. Shafarman, Prog. Photovoltaics **12**, 155 (2004).
[14]S. M. Sze and K. K. Ng, *Physics of Semiconductor Devices*, 3rd ed. (Wiley, New York, 2006).
[15]D. A. R. Barkhouse, O. Gunawan, T. Gokmen, T. K. Todorov, and D. B. Mitzi, Prog. Photovoltaics **20**, 6 (2012).
[16]S. Bag, O. Gunawan, T. Gokmen, Y. Zhu, T. K. Todorov, and D. B. Mitzi, Energy Environ. Sci. **5**, 7060 (2012).
[17]D. B. Mitzi, O. Gunawan, T. K. Todorov, K. Wang, and S. Guha, Sol. Energy Mater. Sol. Cells **95**, 1421 (2011).
[18]I. Repins, M. A. Contreras, B. Egaas, C. DeHart, J. Scharf, C. L. Perkins, B. To, and R. Noufi, Prog. Photovoltaics **16**, 235 (2008).
[19]F. Fabregat-Santiago, G. Garcia-Belmonte, I. Mora-Seró, and J. Bisquert, Phys. Chem. Chem. Phys. **13**, 9083 (2011).
[20]X. Z. Guo, Y. H. Luo, Y. D. Zhang, X. C. Huang, D. M. Li, and Q. B. Meng, Rev. Sci. Instrum. **81**, 103106 (2010).
[21]X. Z. Guo, Y. H. Luo, C. Li, D. Qin, D. M. Li, and Q. B. Meng, Curr. Appl. Phys. **12**, e54 (2012).
[22]M. P. Godlewski, C. R. Baraona, and H. W. Brandhorst, Sol. Cells **29**, 131 (1990).
[23]A. M. Goodman and A. Rose, J. Appl. Phys. **42**, 2823 (1971).
[24]V. D. Mihailetchi, J. Wildeman, and P. W. M. Blom, Phys. Rev. Lett. **94**, 126602 (2005).
[25]L. J. A. Koster, V. D. Mihailetchi, H. Xie, and P. W. M. Blom, Appl. Phys. Lett. **87**, 203502 (2005).
[26]S. D. Stranks, G. E. Eperon, G. Grancini, C. Menelaou, M. J. P. Alcocer, T. Leijtens, L. M. Herz, A. Petrozza, and H. J. Snaith, Science **342**, 341 (2013).
[27]G. Xing, N. Mathews, S. Sun, S. S. Lim, Y. M. Lam, M. Grätzel, S. Mhaisalkar, and T. C. Sum, Science **342**, 344 (2013).
[28]R. Scheer and H.-W. Schock, *Chalcogenide Photovoltaics* (Wiley-VCH Verlag GmbH & Co, KGaA Press, 2011).